Ocean Sci. Discuss., 9, 2749–2792, 2012
www.ocean-sci-discuss.net/9/2749/2012/
doi:10.5194/osd-9-2749-2012

Ocean Science Discussions

OSD
9, 2749–2792, 2012

Export of Arctic freshwater components through the Fram Strait 1998–2010

B. Rabe[1], P. Dodd[2], E. Hansen[2], E. Falck[3], U. Schauer[1], A. Mackensen[1], A. Beszczynska-Möller[1], G. Kattner[1], E. J. Rohling[4], and K. Cox[4]

[1]Alfred Wegener Institute for Polar and Marine Research, Bremerhaven, Germany
[2]Norwegian Polar Institute, Tromso, Norway
[3]The University Centre in Svalbard, Longyearbyen, Norway
[4]National Oceanography Centre, Southampton, UK

Received: 23 July 2012 – Accepted: 26 July 2012 – Published: 14 August 2012

Correspondence to: B. Rabe (benjamin.rabe@awi.de)

Published by Copernicus Publications on behalf of the European Geosciences Union.

Abstract

The East Greenland Current in the Western Fram Strait is an important pathway for liquid freshwater export from the Arctic Ocean to the Nordic Seas and the North Atlantic subpolar gyre. We analysed five hydrographic surveys and data from moored current meters around 79° N in the Western Fram Strait between 1998 and 2010. To estimate the composition of southward liquid freshwater transports, inventories of liquid freshwater and components from Dodd et al. (2012) were combined with transport estimates from an inverse model between 10.6° W and 4° E. The southward liquid freshwater transports through the section averaged to 92 mSv (2900 $km^3 yr^{-1}$), relative to a salinity of 34.9. The transports consisted of 123 mSv water from rivers and precipitation (meteoric water), 28 mSv freshwater from the Pacific and 60 mSv freshwater deficit due to brine from ice formation.

Variability in liquid freshwater and component transports appear to have been partly due to advection of these water masses to the Fram Strait and partly due to variations in the local volume transport; an exception are Pacific Water transports, which showed little co-variability with volume transports. An increase in Pacific Water transports from 2005 to 2010 suggests a release of Pacific Water from the Beaufort Gyre, in line with an observed expansion of Pacific Water towards the Eurasian Basin. The co-variability of meteoric water and brine from ice formation suggests joint processes in the main sea ice formation regions on the Arctic Ocean shelves. In addition, enhanced levels of sea ice melt observed in 2009 likely led to reduced transports of brine from ice formation. At least part of this additional ice melt appears to have been advected from the Beaufort Gyre and from north of the Bering Strait towards the Fram Strait.

The observed changes in liquid freshwater component transports are much larger than known trends in the Arctic liquid freshwater inflow from rivers and the Pacific. Instead, recent observations of an increased storage of liquid freshwater in the Arctic Ocean suggest a decreased export of liquid freshwater. This raises the question how fast the accumulated liquid freshwater will be exported from the Arctic Ocean to the

OSD

9, 2749–2792, 2012

deep water formation regions in the North Atlantic and if an increased export will occur through the Fram Strait.

1 Introduction

As already observed by Nansen (1890), fresh and cold waters from the upper Arctic Ocean are transported southward by the East Greenland Current (EGC) in the Western Fram Strait, over the continental slope and the Greenland shelf (for abbreviations, see the Glossary in Table 1). The EGC transports liquid freshwater (LFW) from the Arctic to the Nordic Seas (e.g. Rudels et al., 2005; Latarius and Quadfasel, 2010), the Denmark Strait and the North Atlantic (Sutherland et al., 2009; Cox et al., 2010). Once in the North Atlantic, this LFW has the potential to influence the deep convection and the thermohaline overturning (Manabe and Stouffer, 1999; Rennermalm et al., 2007; Talley, 2008) as well as the horizontal gyre circulation (Häkkinen, 1999).

1.1 Arctic upper ocean and atmosphere variability

Previous work has shown that the composition of the southward LFW transport in the EGC is influenced not only by processes in the Western Fram Strait but also by the circulation in the Arctic Ocean (Meredith et al., 2001; Dodd et al., 2009; Rabe et al., 2009; Jahn et al., 2010). The pathways of freshwater in the Arctic Ocean and their arrival in the Fram Strait are related to both the large scale atmospheric circulation influencing upper ocean currents and hydrography (Proshutinksy and Johnson, 1997; Steele and Boyd, 1998; Zhang et al., 2003; Häkkinen and Proshutinsky, 2004; Dukhovskoy et al., 2006) as well as regional processes governing the storage and release of LFW.

On basin scales, LFW is stored in and released from the Beaufort Gyre in the Southern Canada Basin but is also advected from the Siberian and Bering Sea shelves to the Fram Strait in the Transpolar Drift. A common conceptual model of upper Arctic Ocean variability entails a switch between strong and weak states of the Beaufort Gyre and

OSD
9, 2749–2792, 2012

the Transpolar Drift on near-decadal timescales (see the review by Mauritzen, 2012). However, the influence of the atmospheric circulation on the Arctic ocean at different timescales is still a subject of ongoing research; in particular, the dominant pattern of large scale atmospheric variability (Thompson and Wallace, 1998; Zhang et al., 2008). In addition, there is evidence of a strong influence of regional atmospheric variability on regional freshwater release and advection; for example, the shelf-basin exchange at the Siberian continental slope (Bauch et al., 2011; Jahn et al., 2010) or Ekman Pumping induced by wind stress in the Amerasian Basin (Rabe et al., 2011).

1.2 Tracers and freshwater in the Arctic Ocean

Different freshwater components have been identified from measurements of salinity and water sample analysis of certain tracers: to separate Pacific Water (PW), the ratio of nitrate to phosphate has been used (Jones et al., 1998; Falck et al., 2005; Yamamoto-Kawai et al., 2006). River water and precipitation (meteoric water, MW) as well as sea ice melt (SIM) and brine from ice formation (IFB) have been distinguished by the isotopic composition of oxygen (Østlund and Hut, 1984; Bauch et al., 1995; Melling and Moore, 1995; Macdonald et al., 1995; Yamamoto-Kawai et al., 2005; Lansard et al., 2012).

By distinguishing the composition of freshwater we are able to gain insight into the links between Arctic-wide freshwater circulation and regional freshwater variability. This includes the release of river water from the Siberian shelves or the release of river water and sea ice melt that previously accumulated in the Beaufort Gyre. Regional ice formation processes also have a strong influence on freshwater inventories by the release of subsurface brine maxima (e.g. Bauch et al., 2009, 2011) from the shelves into the Arctic basins. These brine maxima have been observed to persist within the Transpolar Drift (e.g. Jones et al., 2008a) to ultimately arrive at the Fram Strait.

OSD
9, 2749–2792, 2012

1.3 Liquid freshwater components in the Western Fram Strait

Building on previous work (Bauch et al., 1995; Meredith et al., 2001; Falck et al., 2005; Jones et al., 2008b; Dodd et al., 2009; Rabe et al., 2009), Dodd et al. (2012) estimated the contributions of different water masses to LFW variability around 79° N in the Western Fram Strait between 1998 and 2011.

For the summer sections, inventories of LFW, MW and IFB varied by up to 50 % in time. MW peaked around 2005/2008, related to enhanced levels of MW in the Transpolar Drift following the eastward diversion of MW from the Siberian shelves during the 1990s (Steele and Boyd, 1998). The most PW was found in 1998 and none in 2004 and 2005, which has been linked to temporary changes in the pathways of Pacific Water (Falck et al., 2005) and the strength of the Beaufort Gyre (Proshutinsky et al., 2009). FIFB (freshwater deficit due to IFB) decreased between 1998 and 2011. This may be due to enhanced levels of FSIM (freshwater portion of SIM), indicated by positive values of FSIM near the surface from 2009 onwards.

This study aims to quantify the southward LFW and component transports in the Western Fram Strait for five surveys between 1998 and 2010. We extend the analyses by Rabe et al. (2009) and Dodd et al. (2012) to include PW by considering nutrient measurements in addition to δ^{18}O and salinity. The LFW component fractions by Dodd et al. (2012) are combined with corresponding velocities from an inverse analysis, as described in Sect. 2. The results in Sect. 3 show that levels of MW transports remained similar after 2005, whereas significant southward PW transports were again found in the Western Fram Strait from 2008. The results are discussed in the context of other literature in Sect. 4. We show that changes in the LFW component transports can be linked to Arctic regional processes and large scale circulation, and assume a strong impact on the regions of deep convection in the subpolar North Atlantic gyre. A summary of this study is given in Sect. 5.

2 Data and methods

2.1 Temperature and salinity profiles

Temperature and salinity (CTD) profiles from five ship campaigns between 1998 and 2010 have been used in this study (Table 2) in combination with tracer measurements (Fig. 1a). Several additional CTD profiles were used in the inverse analysis (Sect. 2.4). The hydrographic surveys and instrumentation are described in Fahrbach et al. (2007), Dodd et al. (2012) and the available data links in Table 2.

2.2 Velocity measurements

Velocity was measured during the campaigns using either a vessel-mounted ADCP (vmADCP) or a lowered ADCP (lADCP) along the line of CTD stations (Fig. 1a). The lADCP data were processed using the inverse method by Visbeck (2002). All velocity observations from the ship surveys were detided using predictions from the barotropic Arctic Ocean Tidal Inverse Model (AOTIM-5; Padman and Erofeeva, 2004). This model is only an approximation to the real ocean tides, that, in addition, have a baroclinic component dependent on the bathymetry and ocean stratification. However, the discrepancy between tides in the model and those measured by current meters moored along 79° N in the Fram Strait has been found to be about 0.01 $\mathrm{m\,s^{-1}}$ in the deeper layers of the section but less in the upper layers, where FW is observed (Behrendt, 2008). For the R/V *Polarstern* campaigns, the detided vmADCP profiles were median-averaged to hourly values; standard deviations for the data within each hour were generally below 0.1 $\mathrm{m\,s^{-1}}$. For the R/V *Lance* campaign "Fram Strait 2009", only on-station vmADCP data were used and averaged for each station after detiding; the number of 5 min ensembles available for each station varied from only one to 25. Ship-based velocity observations used in this study are listed by year in Table 3.

In addition, velocity observations from several moored instruments were averaged for the duration of each campaign in the Fram Strait; the moored instruments included both point measurements, such as by Aandera RCM and FSI current meters, and profiles by upward-looking ADCP. Mooring-based velocity observations used in this study are listed by year in Table 3 and are shown in the map in Fig. 1b.

2.3 Tracers and LFW component calculations

Fractions of LFW, PW, SIM and IFB were calculated using an end-member balance (e.g. Ekwurzel et al., 2001; Jones et al., 2008a; Yamamoto-Kawai et al., 2008) with observations of salinity, nitrate, phosphate and oxygen isotope ratio (δ^{18}O) at several CTD profile locations (Fig. 1a). The main difference to previous work (Dodd et al., 2009; Rabe et al., 2009) is the inclusion of nitrate and phosphate observations to add PW to the end-member balance. δ^{18}O for the SIM end-member was set to a constant value, rather than relating it to the surface value of each profile. The salinity of SIM was set to 4 instead of 3. Note that observations from 2004 are used indirectly in this study due to the reconstruction of δ^{18}O values for 2005 from the corresponding relationship to salinity in 2004 (Rabe et al., 2009; Dodd et al., 2012). The data used in this study to obtain LFW and component fractions are a subset of those presented in Dodd et al. (2012) (see their Fig. 2 for data locations); please refer to these authors for further details of tracer measurements and calculation of fractions from an end-member balance.

2.4 Inverse model and water mass transports

We use an inverse analysis model, FEMSECT (Losch et al., 2005), to obtain a physically consistent estimate of meridional velocity and transport from our observations. The model uses the baroclinic thermal wind equation as its physical basis, additionally allowing a non-zero barotropic velocity (Losch et al., 2005; Rabe et al., 2009).

In addition to the shipboard observations from the Fram Strait, time averaged velocity from moored instruments was used in the inverse analysis. Unlike in Rabe et al. (2009), where the average over a whole month close to the ship survey was chosen, we only

OSD
9, 2749–2792, 2012

averaged the velocity over the duration of the survey. Any gaps in the moored instrumental record were filled by linear interpolation in time; these gaps occurred around the time when each mooring was recovered and again deployed. In addition, the near-surface sampling gap in the bottle samples, that did not fill the all of the FEMSECT grid, was filled by constant extrapolation of the topmost transport grid cell. This gap resulted in a maximal underestimate of 5 mSv for southward MW transports, which represents a negligible error. To calculate LFW component transports, each value of a component fraction was linearly interpolated onto the inverse model grid and multiplied by the volume transports in each grid triangle.

The resulting error in the LFW component transports is a combination of the error from the inverse analysis and the error in the LFW component fractions from the end-member equations. From sensitivity analysis of the end-member equations, Dodd et al. (2012) estimated a maximum error of 1 % for MW, 1 % for SIM, 10 % for PW and 10 % for Atlantic Water (AW). As our LFW component transports are based on a subset of the dataset in Dodd et al. (2012), we expect the combined transport error of MW and SIM transports to be almost the same as the error from the inverse estimate. For PW transports, the combined error would be about double the error from the inverse estimate in all years. There is a potential overestimate of MW transports and an underestimate of FSIM transports in 2005 by about 25 % due to the reconstruction of δ^{18}O values from salinity data (see Rabe et al., 2009).

3 Results

3.1 Velocity

The density contours in the inverse solution of our observations (Fig. 2) generally show a front around 3 to 5° W. This front represents the boundary of cold Polar Surface Water in the west and warmer, saltier waters of Atlantic origin in the Central and Eastern Fram Strait (Schlichtholz and Houssais, 2001; Schauer et al., 2004; Beszczynska-

OSD
9, 2749–2792, 2012

Möller et al., 2012). A surface intensified, southward current around the front is evident in our observations in all years, representing the core of the EGC, generally found over the East Greenland continental slope around 3 to 4° W (Fahrbach et al., 2001; Beszczynska-Möller et al., 2012).

Opposing currents occurred in all years, suggesting the presence of horizontal recirculation or eddies (Fig. 2). The density field varied greatly between the different years of observation, leading to different horizontal density gradients and, hence, different geostrophic velocities (not shown) around the core of the EGC: in 2009, horizontal gradients of density were smaller than in the remaining years, leading to lower peak velocities. Strongest horizontal density gradients were evident in 1998 and 2008, due to the presence of a strong meridional recirculation or eddy.

All years of observation show barotropic and baroclinic flows of similar magnitude (Fig. 2), in agreement with previous observational analyses (e.g. Fahrbach et al., 2001) and theoretical considerations regarding the boundary current around the Arctic basins and the Nordic Seas (Aaboe and Nost, 2008; Aaboe et al., 2009). Overall, we expect effects from both atmospheric pressure patterns and bottom density to influence the barotropic flow (e.g. Schlichtholz, 2005). The baroclinic flow is forced by the thickness of the Polar Surface Water layer in the Arctic, via the hydraulically controlled flow in the Fram Strait (e.g. Rudels, 2010) as well as wind induced Ekman transports; however, the latter largely affect the mesoscale variability on timescales of 1–2 months (Jónsson et al., 1992), and little is known about these processes on the shelf in the Western Fram Strait.

3.2 Transports of liquid freshwater and components

3.2.1 Distribution along the section

The meridional transports of all LFW components approximately add up to zero west of 10.6° W in 2005 (see also Rabe et al., 2009). The transports cumulated eastward from this longitude along the section varied strongly between 8° and 3° W (Fig. 3).

This was due to north-/southward alternating currents around the core of the EGC (Fig. 2), where the freshwater inventories were still of similar magnitude as further west (Fig. 9 in Dodd et al., 2012). Further east, the along-section variability was smaller, due to lower inventories. This generally resulted in small increases in transports to about 4° E. The LFW transports in each year reflect the current structure of the velocity sections (Fig. 2) and the distribution of the inventories: opposing transport densities along the section are most noticeable for 2008, whereas the remaining years showed only weak northward LFW transports east of 10.6° W (Fig. 3a). In 2009, a combination of a relatively shallow surface LFW layer (Figs. 7, 10 and 12 in Dodd et al., 2012), and relatively weak velocities (Fig. 2d) and volume transports (Fig. 3e), caused only weak southward LFW transport densities (Fig. 3a).

3.2.2 Average of all years

The integrated LFW transport densities between 10.6° W and 4° E, here termed “section” transports (Fig. 4), averaged to 92 mSv (2900 $km^3 yr^{-1}$, Table 4) for all five years of observation. This is almost the same as the estimate by R09, who only considered 1998, 2004 and 2005; our estimate for two of those years increased due to various changes in the calculation of the inverse volume transports (Sect. 2.4). The average section LFW transport is near the higher end of published transport estimates from observations (Dickson et al., 2007; Serreze et al., 2006) and from high resolution coupled ice-ocean simulations (Jahn et al., 2012). MW transports were about 135 % of LFW transports and FIFB about 65 % (negative FSIM), whereas FPW (freshwater portion of PW) only contributed about 30 %.

3.2.3 Variability

The section LFW transports were similar in almost all years. Only in 2009 they are less than half the maximum, primarily due to weak velocities; in addition, a relatively shallow freshwater layer was observed. Considering year-round observations from moorings only (east of 7° W), the annual mean LFW transports in the Western Fram Strait have not shown any clear trend from 2001 to 2008 (de Steur et al., 2009). According to de Steur et al. the majority of volume transport increases occurred in deeper layers, away from high LFW concentrations. Total transports of MW and FIFB peaked in 2005 (Fig. 3b and c), whereas FPW transports throughout the section were highest in 1998 (Figs. 3d and 4). MW transports followed the minimum in LFW transports in 2009. FIFB transports were only very low in 2009, due to low volume transports and concurrent presence of SIM near the surface and, likely, a reduction of FIFB below by mixing with SIM. After the 2005 minimum, significant FPW transports were observed again in 2008 and 2010, although they may have been lower than our estimate; the reason is a potential overestimate of FPW inventories by the end-member balance used in Dodd et al. (2012) due to processes near the Laptev Sea continental slope (Bauch et al., 2011). However, a large scale model simulation with an ice-ocean coupled general circulation model, the North Atlantic-Arctic Ocean Sea Ice Model (NAOSIM), indicates an increase in the amount of water from the Bering Strait reaching the Fram Strait from 2005 to 2011, with a temporary drop in 2009 (M. Karcher, personal communication, 2012).

3.2.4 Link to volume transports and inventories

From 1998 to 2010, the section transports of LFW and components showed some co-variability both with the volume transports in the upper 300 m (Fig. 5b) and with the section inventories of LFW and components (Fig. 5a). We defined a "section inventory" as the area integral along the section between 10.6° W and 4° E. Whereas LFW inventories changed by up to about 30 % (Fig. 13 in Dodd et al., 2012) the transports were more variable (Fig. 4): in 2005 compared to 1998, we observed higher section inventories of MW as well as only negligible FPW. On the other hand, 2008 shows section inventories of all LFW components larger than or equal to 2005 (Fig. 13, Dodd et al., 2012), opposite to the behavior of MW transports.

OSD
9, 2749–2792, 2012

The correlation coefficients of LFW component transports and the volume transports (Fig. 5a) are around 0.6 for MW and FIFB, but close to zero for FPW. The correlations of LFW component transports and section inventories (Fig. 5b) are around 0.8 and 0.7 for MW and FIFB, respectively, but almost 1 for FPW. LFW transports are correlated to volume transports (0.5) and to LFW inventories (0.6). Significance testing for such short timeseries, with 4 effective degrees of freedom, is not possible; however, we know there must be a relationship between the different quantities, as LFW component transports are the product of the fractions and the velocities. Hence the correlation and visual inspection of Fig. 5 are just an indication of the relative magnitude of the respective relation.

Our results suggests that, not only the presence of LFW components and advection from remote regions but also the ocean dynamics in the Fram Strait are important for the LFW component transports. This is in agreement with model analyses by Jahn et al. (2010) and Lique et al. (2009).

3.2.5 Co-variability of different LFW components

The almost constant LFW transports in four out of the five years of observations suggest that the LFW component transports compensate each other due to processes in the Arctic Ocean. These processes occur both on the large scale, and in regions of origin and storage of the LFW components. The correlation coefficient for volume transports of MW and FIFB is about 0.9, for the corresponding inventories it is about 0.6. This compensation can be represented by the ratio of MW and FIFB transports (Fig. 4). This ratio increased slightly from 3 : 2 in 1998 to 2 : 1 in 2010. The ratio of the section inventories of MW and FIFB showed a similar behavior (Fig. 15 in Dodd et al., 2012).

The presence of significantly positive SIM fractions near the surface in 2009 and 2010, not present in previous years, suggests that some of the IFB signal could have been diluted by additional SIM. Other potential reasons include a change in the production of IFB in the shelf regions or a change in pathways or origin of MW and IFB.

OSD
9, 2749–2792, 2012
Fram Strait freshwater exports 1998–2010
B. Rabe et al.

4 Discussion

4.1 Changes in the Arctic Ocean basins

Our results in Sect. 3.2.4 indicate that not only volume transports influence the LFW component transports, but individual years are strongly affected also by the LFW component fractions in the Fram Strait. This is supported by other studies: the low FPW transports after 1998 have been linked to changes in the extent and the pathways of PW in the Arctic basins; in particular, a climate model simulation has shown that the pathways of PW exports from the Arctic are strongly related to the strength of the Beaufort Gyre (Jahn et al., 2010). Proshutinsky et al. (2009) observed a strong decrease in FPW in the Beaufort Gyre in the 1990s, relative to previous decades, but only a lesser, subsequent reduction until 2007. Concurrently, LFW in the upper mixed layer increased. Proshutinsky et al. linked these processes to the strength of atmospheric cyclonicity in the Arctic through local Ekman Pumping. The strongly anticylonic atmospheric circulation in 2007 suggests that the Beaufort Gyre retained LFW, whereas the anomalously cyclonic winds in 2009 caused a release. On the other hand, Alkire et al. (2007) observed a return of PW in the Central Arctic in 2003/2004 where it had previously been absent since observations began in 2000. The analysis by Alkire et al. also indicated that PW was advected westward along the Siberian continental slope before entering the Transpolar Drift from the East Siberian Sea. They further suggest variability of the PW advection in the Transpolar Drift on timescales of two or more years. The observed return of PW to the Central Arctic and the dynamics of the Beaufort Gyre, implying a storage and release of PW depending on winds, may both have contributed to the advection of PW toward the Fram Strait. This is in line with our observations of increasing PW transports from 2005 to 2010.

The high MW transports in the Fram Strait in 2005 can be linked to strong pulses of river water leaving the Siberian shelves at the end of the 1990s, joining the Transpolar Drift (Anderson et al., 2004; Karcher et al., 2006; Jones et al., 2008a) and reaching the Fram Strait in 2004/2005 (Rabe et al., 2009). Concurrent with our 2005 peak in

MW transports, an anomalously strong pulse of southward LFW transport was also observed on the other side of Greenland, in the Nares Strait (Rabe et al., 2010), suggesting a concurrent large scale advection of MW toward the Arctic export passages. Nevertheless, this pulse does not appear to have drained the Central Arctic of freshwater for the coming years: in 2007 MW was still observed to be high north of the Siberian Islands near the Lomonosov Ridge, compared to observations from the mid-1990s (Abrahamsen et al., 2009). On the Amerasian side, from 1987 to 2007, Yamamoto-Kawai et al. (2009) observed an increase in MW in the center of the Beaufort Gyre. In 2010, the Eurasian Basin (European/Asian side of the Lomonosov Ridge) was observed to be fresher than in 2007/2008, which was attributed to an enhanced import of freshwater from the Beaufort Gyre (Timmermans et al., 2011); this is likely to have contained some of the MW accumulated in the Beaufort Gyre until 2007. Observations of dissolved Barium in 1998 (Taylor et al., 2003) suggest that most of the MW in the Fram Strait originates from Eurasian continental runoff. The above results are in agreement with the persistence of high MW transports after 2005. Much of the additional MW is likely to have originated from Eurasian rivers and advected directly via the Transpolar Drift or via a detour through the Beaufort Gyre.

The co-variability of MW and FIFB transports and inventories (Sect. 3.2.5) may be due to formation processes on the Siberian shelves (Bauch et al., 2009, 2011). Within the Transpolar Drift, Jones et al. (2008a) observed IFB patches at depths below 50 m in the Eurasian Basin, vertically isolated from the much shallower summer surface mixed-layer; furthermore, summer observations in the shelf regions of the Laptev and Kara seas from 1999 to 2001 have shown that waters with salinities lower than 30 take different pathways from the shelf than those with higher salinities (Bauch et al., 2005). Stratification in the upper Arctic Ocean has been found to be enhanced in recent years; for example, Toole et al. (2010) found that even the top 50 m were much more stratified in 2007 than in 1975. This made subsurface temperature maxima inaccessible to surface mixing, at least during summer. Recently, in summer 2011, isolated subsurface temperature maxima have also been observed in the Eurasian Basin during the R/V

OSD
9, 2749–2792, 2012

Polarstern Transarc expedition. This suggests that IFB may be advected in the Transpolar Drift from the Eurasian shelves to the Fram Strait without much modification by SIM near the surface, in particular during the last two decades.

Relative to the 1990s, an ice-ocean coupled general circulation model, NAOSIM, suggests enhanced net sea ice melt (sum of melting and forming of sea ice) on the Siberian shelves and in the region of the Chukchi Plateau, north of the Bering Sea shelf and of the East Siberian Sea shelf, in the time period 2006–2008 (Rabe et al., 2011). SIM has been shown to be rapidly advected from the Siberian shelves to the Fram Strait within the Transpolar Drift (Bauch et al., 2011). In the Central Beaufort Gyre, observations show a reduction in IFB between 1987 and 2007; some additional SIM was observed in 2006 and 2007 (Yamamoto-Kawai et al., 2009). This SIM may have been released from the Beaufort Gyre and partly advected to the Fram Strait, in line with the observed freshening in the Eurasian Basin in 2010 (Timmermans et al., 2011). Hence, we have potential remote sources for the enhanced SIM in the Beaufort Gyre as well as on the Siberian shelves and the resulting decreased FIFB transports we observed in the Fram Strait in 2009/2010. The change in MW to FIFB ratio in the late first decade of the 2000s also suggests a difference in origin of MW and FIFB in the Fram Strait, since MW and IFB have been shown to vary independently in the Canada Basin (Yamamoto-Kawai et al., 2009), unlike on the Siberian shelves (Bauch et al., 2011).

4.2 Changes in LFW imports to the Arctic

In addition to shelf-basin exchange of MW, an increased river discharge is a potential source for increased MW transports in our observations. Overeem and Syvitski (2010) found a 9.8 % increase in annual river discharge over the entire Arctic region from 1977 to 2007; an increase was also found when only data from the 1990s to 2007 were considered. If we consider the Arctic Ocean prior to 1977 to be our reference, the additional river input would have risen by about 0.008 Sv in 30 yr or 0.003 Sv in the 12 yr of our observations in the Fram Strait. However, this increase is well below the variability in MW transports that we observe. Hence, trends in river discharge are negligible with respect to the changes in MW transports in the Fram Strait between 1998 and 2010.

Changes in PW transports through the Fram Strait could potentially be due to changes in the Arctic inflow of PW. However, the observed LFW transport through the Bering Strait shows no trend from 1998 to 2004 (Woodgate et al., 2006) and preliminary analysis shows no trend from 1998 to 2009; nevertheless, theses analyses have not yet accounted for transport by the Alaskan Coastal Current (R. Woodgate, personal communication, 2011). Estimates from model simulations put the transit times of PW from the Bering Strait to the Fram Strait at around 5 to 10 yr (Nguyen et al., 2011), in line with observational estimates for PW residence time in the Canada Basin (11 ± 4 yr Yamamoto-Kawai et al., 2008). Therefore, any Bering Strait signal arriving in the Fram Strait in 1998 would have to have been generated around 1990, prior to the start of continuous records by moored observatories. However, we can conclude that the increased spreading of PW and our observed FPW transport increase after 2005 are not likely due to increased import through the Bering Strait. It is more likely that PW was diverted onto the Siberian shelves and subsequently released into the basins around 2004, as indicated by Alkire et al. (2007).

4.3 Dynamics and surface forcing

Changes in the large scale circulation are reflected in the transports we observe in the Western Fram Strait. This may be due to direct atmospheric forcing, for example, winds in the Fram Strait or sea surface height forced by sea level pressure within the region. Furthermore, high levels of LFW from remote regions may be advected toward the Fram Strait; for example, from the Amerasian Basin or from the Eurasian shelves via the Transpolar Drift.

As an indicator of changes in the atmospheric circulation, we compare our results to the Arctic Oscillation (AO; Thompson and Wallace, 1998), denoting the pressure difference between temperate latitudes over the Atlantic and the Arctic high. The AO was generally positive during most of the 1990s (weak Arctic high; see Fig. 6), influencing the upper ocean stratification and LFW pathways in the Eurasian Basin (e.g. Steele and Boyd, 1998). Subsequently, the AO switched to a predominantly negative state (strong Arctic high), although it alternated to weakly positive states on timescales of 2 to 3 yr until about 2009/2010, when it became strongly negative.

We have shown that transports of LFW show a similarly high correlation with the corresponding inventories and with the volume transports, whereas for MW and FIFB the correlation with inventories is stronger. The LFW and component section transports are, therefore, a mixture of the different influences from local ocean dynamics as well as advection of LFW components from remote areas; the exception is PW, which is not linearly related to volume transport changes, as PW variability is dominated by the strong inventory change after 1998.

We would expect significant fluctuations in volume transports on shorter than annual timescales as a response to regional sea level pressure changes. Hence, correlating volume transports with the AO or regional sea level pressure changes would require analysing the timeseries of moored observations, which is beyond the scope of this work. However, Fig. 6 suggests that volume transports were generally low when the AO in the previous year was near zero or positive, whereas after noticeably negative AO years (2005 and 2010), volume transports almost doubled.

The Eurasian Basin was observed to be fresher in 2010 than in 2007/2008, which was attributed to an enhanced import of freshwater from the Beaufort Gyre (Timmermans et al., 2011) due to a temporarily anomalous cyclonic circulation in the Arctic atmosphere (see the negative AO index in 2009 and 2010; Fig. 6). This increase in LFW north of the Fram Strait could have increased the layer thickness of freshwater north of the Fram Strait and may have forced an enhanced baroclinic transport (e.g. Rudels, 2010) of LFW through the Fram Strait in 2010; in addition, the LFW increase could have supplied the increased LFW transports even without changes in Fram Strait volume transports.

OSD
9, 2749–2792, 2012

4.4 Canadian Arctic Archipelago exports and circulation at lower latitudes

A peak in MW and SIM was observed in the EGC in the Denmark Strait in 2005, relative to observations in 2004 and 2008 (Cox et al., 2010). Cox et al. attribute this observation to an enhanced export of sea ice in the EGC through the Fram Strait. Our observations also show peaks in the transports of MW and IFB in 2005, which would influence the signal arriving in the Denmark Strait. The advective timescale in the EGC from the Fram Strait to the Denmark Strait has been estimated to be of the order of a few months (Dodd et al., 2009). Hence, our transport results indicate that the MW and SIM peak found in the Denmark Strait in 2005 is at least to some extent due to changes in the LFW transport composition in the Fram Strait. Furthermore, Sutherland et al. (2009) found high levels of PW in the vicinity of the Denmark Strait during the 1990s and a decline to much lower levels in 2002 and 2004. They related these levels of PW to the AO, which is in agreement with our transport analysis.

The observed LFW transports through the Western Fram Strait showed no clear trend between 1998 and 2008 (Rabe et al., 2009; de Steur et al., 2009, this study). The export of LFW from the Arctic Ocean through the Canadian Arctic Archipelago also reaches the North Atlantic (Labrador Sea) via the Davis Strait. Here, observations and model simulations show a decrease in the southward LFW transport from 2004 to 2008, and the simulations showed overall decreasing levels of transports from the 1990s to 2004 (P. Holliday, personal communication, 2012). The study further supported decreasing LFW transports by salinity measurements on the Newfoundland and Labrador shelf as well as by a hydrographic survey across the Labrador Sea in 2008. The NAOSIM simulation showed a decrease in net Arctic LFW exports since the 1990s (M. Karcher, personal communication, 2012). These findings are in agreement with a recently detected increase in LFW storage in the upper Arctic Ocean (Rabe et al., 2011). It remains to be seen if this additional LFW will be released to the North Atlantic in the near future and how this export will be distributed between the different passages.

5 Summary

We present more than a decade of observed LFW and component inventories and corresponding southward transports in the Western Fram Strait. The transports were derived using LFW component fractions from δ^{18}O and nutrient observations (Dodd et al., 2012) together with velocities from an inverse model; the latter combines five hydrographic/velocity sections from observational campaigns between 1998 and 2010 as well as concurrent records from moored instruments.

- On average for all five sections, we observed a southward LFW transport between 11° W and 4° E of 92 mSv (2900 km^3 yr^{-1}), relative to a salinity of 34.9. The LFW transport consisted of 123 mSv (3880 km^3 yr^{-1}) MW, 60 mSv (–1890 km^3 yr^{-1}) freshwater deficit due to IFB (negative SIM), and 330 mSv (10 390 km^3 yr^{-1}) PW transport, containing 28 mSv (870 km^3 yr^{-1}) freshwater.

- LFW and component transports are correlated with both changes in the amount of LFW present in the Fram Strait (inventories) and changes in volume transports; the exception are PW transports, which only co-varied with inventory changes. PW transports were likely influenced by advection from other regions of the Arctic Ocean, primarily the Beaufort Gyre. On the other hand, MW and IFB transports were likely related to changes in local volume transports and to LFW release near the Siberian shelves.

- We find that section transports of MW and IFB covary in time, as do the corresponding inventories. This suggests joint processes of these water masses in the production regions of IFB and concurrent pathways through the Arctic Ocean before arriving at the Fram Strait. Increased stratification observed in the Amerasian and Eurasian Arctic in the first decade of the 2000s suggests that IFB may generally be advected from the Siberian shelves in the Transpolar Drift to the Fram Strait with little or no alteration by surface processes.

- We observed an increase in the ratio of MW to IFB transports in time. This was possibly due to to enhanced levels of SIM in 2009 and 2010. At least some of this additional SIM was likely advected into the Fram Strait from the Beaufort Gyre and from the region north of the Bering Strait. Furthermore, changes in the advective pathways and in the production region of IFB on the Siberian shelves may have influenced the ratio.
- Comparison to other analyses indicates that the changes in LFW component transports we observed in the Fram Strait are much larger than known trends in the Arctic LFW inflow from rivers and the Pacific. Recent observations of increasing LFW storage in the Arctic Ocean since the 1990s suggest, instead, a decreased export of LFW. We observed no trend in Arctic LFW export through the upper Western Fram Strait between 1998 and 2010; instead, a reduction in LFW export has been indicated by observations on the western side of Greenland (P. Holliday, personal communication, 2012).

  This raises the question how fast the accumulated LFW will be exported in the future, ultimately to the deep water formation regions of the North Atlantic, and if an increased export will occur through the Fram Strait.

Appendix A

List of velocity datasets from moorings

This section lists the sources for the velocity datasets from the moorings in the Eastern Fram Strait. The corresponding citations are arranged by the respective year associated with our transport estimates:

- 1998

  Fahrbach, E; Rohardt, G; Schauer, U (2012): physical oceanography and current meter data from mooring F1-2 doi:10.1594/PANGAEA.778887

OSD
9, 2749–2792, 2012
Fram Strait freshwater exports 1998–2010
B. Rabe et al.

Fahrbach, E; Rohardt, G; Schauer, U (2012): physical oceanography and current meter data from mooring F1-1 doi:10.1594/PANGAEA.778886

Fahrbach, E; Rohardt, G; Schauer, U (2012): physical oceanography and current meter data from mooring F2-1 doi:10.1594/PANGAEA.778898

Fahrbach, E; Rohardt, G; Schauer, U (2012): physical oceanography and current meter data from mooring F2-2 doi:10.1594/PANGAEA.778899

Fahrbach, E; Rohardt, G; Schauer, U (2012): physical oceanography and current meter data from mooring F3-1 doi:10.1594/PANGAEA.778904

Fahrbach, E; Rohardt, G; Schauer, U (2012): physical oceanography and current meter data from mooring F3-2 doi:10.1594/PANGAEA.778905

Fahrbach, E; Rohardt, G; Schauer, U (2012): physical oceanography and current meter data from mooring F4-1 doi:10.1594/PANGAEA.778909

Fahrbach, E; Rohardt, G; Schauer, U (2012): physical oceanography and current meter data from mooring F4-2 doi:10.1594/PANGAEA.778910

Fahrbach, E; Rohardt, G; Schauer, U (2012): physical oceanography and current meter data from mooring F5-1 doi:10.1594/PANGAEA.778914

Fahrbach, E; Rohardt, G; Schauer, U (2012): physical oceanography and current meter data from mooring F5-2 doi:10.1594/PANGAEA.778915

Fahrbach, E; Rohardt, G; Schauer, U (2012): physical oceanography and current meter data from mooring F6-1 doi:10.1594/PANGAEA.778919

Fahrbach, E; Rohardt, G; Schauer, U (2012): physical oceanography and current meter data from mooring F6-2 doi:10.1594/PANGAEA.778920

Fahrbach, E; Rohardt, G; Schauer, U (2012): physical oceanography and current meter data from mooring F7-1 doi:10.1594/PANGAEA.778925

Fahrbach, E; Rohardt, G; Schauer, U (2012): physical oceanography and current meter data from mooring F7-2 doi:10.1594/PANGAEA.778926

OSD

9, 2749–2792, 2012

Fram Strait freshwater exports 1998–2010

B. Rabe et al.

Fahrbach, E; Rohardt, G; Schauer, U (2012): physical oceanography and current meter data from mooring F8-1 doi:10.1594/PANGAEA.778930

Fahrbach, E; Rohardt, G; Schauer, U (2012): physical oceanography and current meter data from mooring F8-2 doi:10.1594/PANGAEA.778931

– 2005

Beszczynska-Möller, A; Fahrbach, E; Rohardt, G et al. (2012): physical oceanography and current meter data from mooring F1-8 doi:10.1594/PANGAEA.778857

Beszczynska-Möller, A; Fahrbach, E; Rohardt, G et al. (2012): physical oceanography and current meter data from mooring F1-7 doi:10.1594/PANGAEA.778856

Beszczynska-Möller, A; Fahrbach, E; Rohardt, G et al. (2012): physical oceanography and current meter data from mooring F10-7 doi:10.1594/PANGAEA.778859

Beszczynska-Möller, A; Fahrbach, E; Rohardt, G et al. (2012): physical oceanography and current meter data from mooring F15-3 doi:10.1594/PANGAEA.778861

Beszczynska-Möller, A; Fahrbach, E; Rohardt, G et al. (2012): physical oceanography and current meter data from mooring F15-4 doi:10.1594/PANGAEA.778862

Beszczynska-Möller, A; Fahrbach, E; Rohardt, G et al. (2012): physical oceanography and current meter data from mooring F16-4 doi:10.1594/PANGAEA.778865

Beszczynska-Möller, A; Fahrbach, E; Rohardt, G et al. (2012): physical oceanography and current meter data from mooring F16-3 doi:10.1594/PANGAEA.778864

Beszczynska-Möller, A; Fahrbach, E; Rohardt, G et al. (2012): physical oceanography and current meter data from mooring F2-8 doi:10.1594/PANGAEA.778867

Beszczynska-Möller, A; Fahrbach, E; Rohardt, G et al. (2012): physical oceanography and current meter data from mooring F2-9 doi:10.1594/PANGAEA.778868

Beszczynska-Möller, A; Fahrbach, E; Rohardt, G et al. (2012): physical oceanography and current meter data from mooring F3-7 doi:10.1594/PANGAEA.778869

OSD

9, 2749–2792, 2012

Fram Strait freshwater exports 1998–2010

B. Rabe et al.

Beszczynska-Möller, A; Fahrbach, E; Rohardt, G et al. (2012): physical oceanography and current meter data from mooring F3-8 doi:10.1594/PANGAEA.778870

Beszczynska-Möller, A; Fahrbach, E; Rohardt, G et al. (2012): physical oceanography and current meter data from mooring F4-7 doi:10.1594/PANGAEA.778872

Beszczynska-Möller, A; Fahrbach, E; Rohardt, G et al. (2012): physical oceanography and current meter data from mooring F4-8 doi:10.1594/PANGAEA.778873

Beszczynska-Möller, A; Fahrbach, E; Rohardt, G et al. (2012): physical oceanography and current meter data from mooring F5-7 doi:10.1594/PANGAEA.778875

Beszczynska-Möller, A; Fahrbach, E; Rohardt, G et al. (2012): physical oceanography and current meter data from mooring F5-8 doi:10.1594/PANGAEA.778876

Beszczynska-Möller, A; Fahrbach, E; Rohardt, G et al. (2012): physical oceanography and current meter data from mooring F6-9 doi:10.1594/PANGAEA.778879

Beszczynska-Möller, A; Fahrbach, E; Rohardt, G et al. (2012): physical oceanography and current meter data from mooring F6-8 doi:10.1594/PANGAEA.778878

Beszczynska-Möller, A; Fahrbach, E; Rohardt, G et al. (2012): physical oceanography and current meter data from mooring F7-6 doi:10.1594/PANGAEA.778880

Beszczynska-Möller, A; Fahrbach, E; Rohardt, G et al. (2012): physical oceanography and current meter data from mooring F7-7 doi:10.1594/PANGAEA.778881

Beszczynska-Möller, A; Fahrbach, E; Rohardt, G et al. (2012): physical oceanography and current meter data from mooring F8-8 doi:10.1594/PANGAEA.778883

Beszczynska-Möller, A; Fahrbach, E; Rohardt, G et al. (2012): physical oceanography and current meter data from mooring F8-7 doi:10.1594/PANGAEA.778882

Beszczynska-Möller, A; Fahrbach, E; Rohardt, G et al. (2012): physical oceanography and current meter data from mooring F9-6 doi:10.1594/PANGAEA.778884

Beszczynska-Möller, A; Fahrbach, E; Rohardt, G et al. (2012): physical oceanography and current meter data from mooring F9-7 doi:10.1594/PANGAEA.778885

– 2008

Beszczynska-Möller, A; Fahrbach, E; Schauer, U (2012): physical oceanography and current meter data from mooring F1-10 doi:10.1594/PANGAEA.777564

Beszczynska-Möller, A; Fahrbach, E; Schauer, U (2012): physical oceanography and current meter data from mooring F10-9 doi:10.1594/PANGAEA.777567

Beszczynska-Möller, A; Fahrbach, E; Schauer, U (2012): physical oceanography and current meter data from mooring F15-6 doi:10.1594/PANGAEA.777569

Beszczynska-Möller, A; Fahrbach, E; Schauer, U (2012): physical oceanography and current meter data from mooring F16-6 doi:10.1594/PANGAEA.777572

Beszczynska-Möller, A; Fahrbach, E; Schauer, U (2012): physical oceanography and current meter data from mooring F2-11 doi:10.1594/PANGAEA.777575

Beszczynska-Möller, A; Fahrbach, E; Schauer, U (2012): physical oceanography and current meter data from mooring F3-10 doi:10.1594/PANGAEA.777579

Beszczynska-Möller, A; Fahrbach, E; Schauer, U (2012): physical oceanography and current meter data from mooring F4-10 doi:10.1594/PANGAEA.777584

Beszczynska-Möller, A; Fahrbach, E; Schauer, U (2012): physical oceanography and current meter data from mooring F5-10 doi:10.1594/PANGAEA.777589

Beszczynska-Möller, A; Fahrbach, E; Schauer, U (2012): physical oceanography and current meter data from mooring F6-11 doi:10.1594/PANGAEA.777595

Beszczynska-Möller, A; Fahrbach, E; Schauer, U (2012): physical oceanography and current meter data from mooring F7-8 doi:10.1594/PANGAEA.777600

Beszczynska-Möller, A; Fahrbach, E; Schauer, U (2012): physical oceanography and current meter data from mooring F9-8 doi:10.1594/PANGAEA.777605

Beszczynska-Möller, A; Fahrbach, E; Schauer, U (2012): physical oceanography and current meter data from mooring F8-9 doi:10.1594/PANGAEA.777604

OSD
9, 2749–2792, 2012

– 2009

Beszczynska-Möller, A; Fahrbach, E; Schauer, U (2012): physical oceanography and current meter data from mooring F10-10 doi:10.1594/PANGAEA.777566

Beszczynska-Möller, A; Fahrbach, E; Schauer, U (2012): physical oceanography and current meter data from mooring F15-7 doi:10.1594/PANGAEA.777570

Beszczynska-Möller, A; Fahrbach, E; Schauer, U (2012): physical oceanography and current meter data from mooring F16-7 doi:10.1594/PANGAEA.777573

Beszczynska-Möller, A; Fahrbach, E; Schauer, U (2012): physical oceanography and current meter data from mooring F2-13 doi:10.1594/PANGAEA.777577

Beszczynska-Möller, A; Fahrbach, E; Schauer, U (2012): physical oceanography and current meter data from mooring F3-12 doi:10.1594/PANGAEA.777581

Beszczynska-Möller, A; Fahrbach, E; Schauer, U (2012): physical oceanography and current meter data from mooring F4-12 doi:10.1594/PANGAEA.777586

Beszczynska-Möller, A; Fahrbach, E; Schauer, U (2012): physical oceanography and current meter data from mooring F5-12 doi:10.1594/PANGAEA.777591

Beszczynska-Möller, A; Fahrbach, E; Schauer, U (2012): physical oceanography and current meter data from mooring F6-13 doi:10.1594/PANGAEA.777597

Beszczynska-Möller, A; Fahrbach, E; Schauer, U (2012): physical oceanography and current meter data from mooring F7-9 doi:10.1594/PANGAEA.777601

Beszczynska-Möller, A; Fahrbach, E; Schauer, U (2012): physical oceanography and current meter data from mooring F8-10 doi:10.1594/PANGAEA.777602

Beszczynska-Möller, A; Fahrbach, E; Schauer, U (2012): physical oceanography and current meter data from mooring F9-9 doi:10.1594/PANGAEA.777606

– 2010

Beszczynska-Möller, A; Fahrbach, E; Schauer, U (2012): physical oceanography and current meter data from mooring F2-14 doi:10.1594/PANGAEA.777578

OSD

9, 2749–2792, 2012

Fram Strait freshwater exports 1998–2010

B. Rabe et al.

Beszczynska-Möller, A; Fahrbach, E; Schauer, U (2012): physical oceanography and current meter data from mooring F3-13 doi:10.1594/PANGAEA.777582

Beszczynska-Möller, A; Fahrbach, E; Schauer, U (2012): physical oceanography and current meter data from mooring F4-13 doi:10.1594/PANGAEA.777587

Beszczynska-Möller, A; Fahrbach, E; Schauer, U (2012): physical oceanography and current meter data from mooring F5-13 doi:10.1594/PANGAEA.777592

Beszczynska-Möller, A; Fahrbach, E; Schauer, U (2012): physical oceanography and current meter data from mooring F7-10 doi:10.1594/PANGAEA.777599

Beszczynska-Möller, A; Fahrbach, E; Schauer, U (2012): physical oceanography and current meter data from mooring F6-14 doi:10.1594/PANGAEA.777598

Beszczynska-Möller, A; Fahrbach, E; Schauer, U (2012): physical oceanography and current meter data from mooring F8-11 doi:10.1594/PANGAEA.777603

Acknowledgements. We thank all the scientists and crew of the different survey campaigns that contributed to this work. This work was supported by the Co-Operative Project "The North Atlantic as Part of the Earth System: From System Comprehension to Analysis of Regional Impacts" funded by the German Federal Ministry for Education and Research (BMBF), project #03F0605E . Paul Dodd was funded by the Norwegian Research Council under the IPY project IAOOS Norway. This study contributes to UK Natural Environment Research Council project NER/T/S/2002/00453.

References

Aaboe, S. and Nost, O. A.: A diagnostic model of the nordic seas and Arctic Ocean circulation: quantifying the effects of a variable bottom density along a sloping topography, J. Phys. Oceanogr., 38, 2685–2703, doi:10.1175/2008JPO3862.1, 2008. 2757

Aaboe, S., Nost, O. A., and Hansen, E.: Along-slope variability of barotropic transport in the nordic seas: simplified dynamics tested against observations, J. Geophys. Res., 114, C03009, doi:10.1029/2008JC005094, 2009. 2757

Abrahamsen, E. P., Meredith, M. P., Falkner, K. K., Torres-Valdes, S., Leng, M. J., Alkire, M. B., Bacon, S., Laxon, S. W., Polyakov, I., and Ivanov, V.: Tracer-derived freshwater composition of the Siberian continental shelf and slope following the extreme Arctic summer of 2007, Geophys. Res. Lett., 36, L07602, doi:10.1029/2009GL037341, 2009. 2762

Alkire, M. B., Falkner, K. K., Rigor, I., Steele, M., and Morison, J.: The return of Pacific waters to the upper layers of the Central Arctic Ocean, Deep-Sea Res. Pt. I, 54, 1509–1529, 2007. 2761, 2764

Anderson, L. G., Jutterström, S., Kaltin, S., Jones, E. P., and Björk, G.: Variability in river runoff distribution in the Eurasian Basin of the Arctic Ocean, J. Geophys. Res.,109, C01016, 109, doi:10.1029/2003JC001773, 2004. 2761

Bauch, D., Schlosser, P., and Fairbanks, R. G.: Freshwater balance and the sources of deep and bottom waters in the Arctic Ocean inferred from the distribution of $H_2^{18}O$, Prog. Oceanogr., 35, 53–80, 1995. 2752, 2753

Bauch, D., Erlenkeuser, H., and Andersen, N.: Water mass processes on Arctic shelves as revealed from $\delta^{18}O$ of H_2O, Global Planet. Change, 48, 165–174, 2005. 2762

Bauch, D., Dmitrenko, I. A., Hölemann, J., Kirillov, S. A., and Kassens, H.: Exchange of Laptev Sea and Arctic Ocean halocline waters in response to atmospheric forcing, J. Geophys. Res. ,114, C05008, doi:10.1029/2008JC005062, 2009. 2752, 2762

Bauch, D., Gröger, M., Dmitrenko, I., Hölemann, J., Kirillov, S., Mackensen, A., Taldenkova, E., and Andersen, N.: Atmospheric controlled freshwater release at the Laptev Sea continental margin, Polar Res., 30, 5858, doi:10.3402/polar.v30i0.5858, 2011a. 2752, 2762

Bauch, D., van der Loeff, M. R., Andersen, N., Torres-Valdes, S., Bakker, K., and Abrahamsen, E. P.: Origin of freshwater and polynya water in the Arctic Ocean halocline in summer 2007, Prog. Oceanogr., 91, 482–495, doi:10.1016/j.pocean.2011.07.017, 2011b. 2759, 2763

Behrendt, A.: Comparison of the Current Field in Fram Strait derived from ADCP Measurements and Mooring Data, Master's thesis, University of Bremen, Bremen, Germany, 2008. 2754

Beszczynska-Möller, A. and Wisotzki, A.: Physical Oceanography during POLARSTERN Cruise ARK-XXIII/2, Alfred Wegener Institute for Polar and Marine Research, Bremerhaven, doi:10.1594/PANGAEA.733424, 2010. 2784, 2785

Beszczynska-Möller, A., Fahrbach, E., Schauer, U., and Hansen, E.: Variability in Atlantic water temperature and transport at the entrance to the Arctic Ocean, 1997–2010, ICES J. Mar. Sci., 69, 852–863 doi:10.1093/icesjms/fss056, 2012. 2756, 2757, 2785

Cox, K. A., Stanford, J. D., McVicar, A. J., Rohling, E. J., Heywood, K. J., Bacon, S., Bolshaw, M., Dodd, P. A., De la Rosa, S., and Wilkinson, D.: Interannual variability of Arctic sea ice export into the East Greenland Current, J. Geophys. Res., 115, C12063, doi:10.1029/2010JC006227, 2010. 2751, 2766

de Steur, L., Hansen, E., Gerdes, R., Karcher, M., Fahrbach, E., and Holfort, J.: Freshwater fluxes in the East Greenland Current: a decade of observations, Geophys. Res. Lett., 36, L23611, doi:10.1029/2009GL041278, 2009. 2759, 2766

Dickson, R., Rudels, B., Dye, S., Karcher, M., Meincke, J., and Yashayaev, I.: Current estimates of freshwater flux through Arctic and subarctic seas, Prog. Oceanogr., 73, 210–230, doi:10.1016/j.pocean.2006.12.003, 2007. 2758

Dodd, P. A., Heywoiod, K. J., Meredith, M. P., Naveira-Garabato, A. C., Marca, A. D., and Falkner, K. K.: Sources and fate of freshwater exported in the East Greenland current, Geophys. Res. Lett., 36, L19608, doi:10.1029/2009GL039663, 2009. 2751, 2753, 2755, 2766

Dodd, P., Rabe, B., Hansen, E., Falck, E., Mackensen, A., Rohling, E., Stedmon, C., and Kistiansen, S.: The freshwater composition of the Fram Strait outflow derived from a decade of tracer measurements, under review at J. Geophys. Res. Oceans, 2012. 2750, 2753, 2754, 2755, 2756, 2758, 2759, 2760, 2767, 2784, 2787, 2791

Dukhovskoy, D., Johnson, M., and Proshutinsky, A.: Arctic decadal variability from an idealized atmosphere-ice-ocean model: 2. Simulation of decadal oscillations, J. Geophys. Res., 111, C06029, doi:10.1029/2004JC002820, 2006. 2751

Ekwurzel, B., Schlosser, P., Mortlock, R. A., and Fairbanks, R. G.: River runoff, sea ice meltwater, and Pacific water distribution and mean residence times in the Arctic Ocean, J. Geophys. Res., 106, 9075–9092, 2001. 2755

Fahrbach, E.: Shipboard acoustic doppler current profiling during cruise ARK-XIV/2a, SAC ID 00493, Alfred Wegener Institute for Polar and Marine Research, Bremerhaven, doi:10.1594/PANGAEA.318314, available at: http://store.pangaea.de/Projects/WOCE/SADCP/PS52_00493.pdf (last access: 1 August 2012), 2005. 2785

Fahrbach, E. and VEINS members: Hydrochemistry measured on water bottle samples during POLARSTERN cruise ARK-XIV/2, Alfred Wegener Institute for Polar and Marine Research, Bremerhaven, doi:10.1594/PANGAEA.759130, 2010. 2784

Fahrbach, E., Meincke, J., Østerhus, S., Rohardt, G., Schauer, U., Tverberg, V., and Verduin, J.: Direct measurements of volume transports through Fram Strait, Polar Res., 20, 217–224, 2001. 2757, 2785

Fahrbach, E., Rohardt, G., and Sieger, R. (eds.): 25 Years of POLARSTERN Hydrography (1982–2007), Alfred Wegener Institute for Polar and Marine Research, Bremerhaven, doi:10013/epic.30213.d001, 2007. 2754

Falck, E., Kattner, G., and Budèus, G.: Disappearance of Pacific water in the Northwestern Fram Strait, Geophys. Res. Lett., 32, L14619, 32, doi:10.1029/2005GL023400, 2005. 2752, 2753

Häkkinen, S.: A simulation of the thermohaline effects of a great salinity anomaly, J. Climate, 12, 1781–1795, 1999. 2751

Häkkinen, S. and Proshutinsky, A.: Freshwater content variability in the Arctic Ocean, J. Geophys. Res., 109, C03051, doi:10.1029/2003JC001940, 2004. 2751

Jahn, A., Tremblay, L. B., Newton, R., Holland, M. M., Mysak, L. A., and Dmitrenko, I. A.: A tracer study of the Arctic Ocean's liquid freshwater export variability, J. Geophys. Res., 115, C07015, doi:10.1029/2009JC005873, 2010. 2751, 2752, 2760, 2761

Jahn, A., Aksenov, Y., de Cuevas, B., de Steur, L., Hakkinen, S., Hansen, E., Herbaut, C., Houssais, M.-N., Karcher, M. J., Kauker, F., Lique, C., Nguyen, A. T., Pemberton, P., Worthen, D. L., and Zhang, J.: Arctic Ocean freshwater – How robust are model simulations?, J. Geophys. Res., doi:10.1029/2012JC007907, in press, 2012. 2758

Jakobsson, M., Macnab, R., Mayer, M., Anderson, R., Edwards, M., Hatzky, J., Schenke, H.-W., and Johnson, P.: An improved bathymetric portrayal of the Arctic Ocean: implications for ocean modeling and geological, geophysical and oceanographic analyses, Geophys. Res. Lett., 35, L07602, doi:10.1029/2008GL033520, 2008. 2787

Jones, E. P., Anderson, L. G., and Swift, J. H.: Distribution of Atlantic and Pacific waters in the upper Arctic Ocean: implications for circulation, Geophys. Res. Lett., 25, 765–768, 1998. 2752

Jones, E. P., Anderson, L. G., Jutterström, S., Mintrop, L., and Swift, J. H.: Pacific fresh water, river water and sea ice meltwater across Arctic Ocean basins: results from the 2005 Beringia Expedition, J. Geophys. Res., 113, C08012, doi:10.1029/2007JC004124, 2008a. 2752, 2755, 2761, 2762

Jones, E. P., Anderson, L. G., Jutterström, S., and Swift, J. H.: Sources and distribution of freshwater in the East Greenland Current, Prog. Oceanogr., 78, 37–44, doi:10.1016/j.pocean.2007.06.003, 2008b. 2753

Jónsson, S., Foldvik, A., and Aagaard, K.: The structure and atmospheric forcing of the mesoscale velocity field in Fram Strait, J. Geophys. Res., 97, 12585–12600, 1992. 2757

Karcher, M., Gerdes, R., and Kauker, F.: Modeling of $\delta^{18}O$ and ^{99}Tc dispersion in Arctic and subarctic seas, ASOF Newsl., 5, available from: http://asof.npolar.no (last access: 1 August 2012), unpublished manuscript, 2006. 2761

Lansard, B., Mucci, A., Miller, L. A., Macdonald, R. W., and Gratton, Y.: Seasonal variability of water mass distribution in the Southeastern Beaufort Sea determined by total alkalinity and $\delta^{18}O$, J. Geophys. Res., 117, C03003, doi:10.1029/2011JC007299, 2012. 2752

Latarius, K. and Quadfasel, D.: Seasonal to inter-annual variability of temperature and salinity in the Greenland Sea gyre: heat and freshwater budgets, Tellus A, 62, 497–515, doi:10.1111/j.1600-0870.2010.00453.x, 2010. 2751

Lique, C., Treguier, A. M., Scheinert, M., and Penduff, T.: A model-based study of ice and freshwater transport variability along both sides of Greenland, Clim. Dynam., 33, 685–705, doi:10.1007/s00382-008-0510-7, 2009. 2760

Losch, M., Sidorenko, D., and Beszczynska-Möller, A.: FEMSECT: an inverse section model based on the finite element method, J. Geophys. Res., 110, C12023, doi:10.1029/2005JC002910, 2005. 2755

Macdonald, R., Paton, D., Carmack, E., and Omstedt, A.: The fresh-water budget and under-ice spreading of Mackenzie River water in the Canadian Beaufort Sea based on salinity and $\delta^{18}O/\delta^{16}O$ measurements in water and ice, J. Geophys. Res.-Oceans, 100, 895–919, doi:10.1029/94JC02700, 1995. 2752

Manabe, S. and Stouffer, R. J.: The role of thermohaline circulation in climate, Tellus A, 51, 91–109, 1999. 2751

Mauritzen, C.: Oceanography: arctic freshwater, Nat. Geosci., 5, 162–164, doi:10.1038/ngeo1409, 2012. 2752

Melling, H. and Moore, R. M.: Modification of halocline source waters during freezing on the Beaufort Sea shelf: evidence from oxygen isotopes and dissolved nutrients, Cont. Shelf. Res., 15, 89–113, 1995. 2752

Meredith, M., Heywood, K., Dennis, P., Goldson, L., White, R., Fahrbach, E., Schauer, U., and Østerhus, S.: Freshwater fluxes through the Western Fram Strait, Geophys. Res. Lett., 28, 1615–1618, 2001. 2751, 2753

Nansen, F.: The First Crossing of Greenland, Longmans, Green, translated by Hubert M. Gepp. London, 1890. 2751

Nguyen, A. T., Menemenlis, D., and Kwok, R.: Arctic ice-ocean simulation with optimized model parameters: approach and assessment, J. Geophys. Res., 116, C04025, doi:10.1029/2010JC006573, 2011. 2764

Østlund, H. G. and Hut, G.: Arctic Ocean water mass balance from isotope data, J. Geophys. Res., 89, 6373–6381, 1984. 2752

Overeem, I. and Syvitski, J. P. M.: Shifting discharge peaks in Arctic rivers, 1977–2007, Geogr. Ann. A, 92, 285–296, 2010. 2763

Padman, L. and Erofeeva, S.: A barotropic inverse tidal model for the Arctic Ocean, Geophys. Res. Lett., 31, L02303, doi:10.1029/2003GL019003, 2004. 2754

Proshutinksy, A. Y. and Johnson, M. A.: Two circulation regimes of the wind-driven Arctic Ocean, J. Geophys. Res., 102, 12493–12514, 1997. 2751

Proshutinsky, A., Krishfield, R., Timmermans, M.-L., Toole, J., Carmack, E., McLaughlin, F., Williams, W. J., Zimmermann, S., Itoh, M., and Shimada, K.: Beaufort gyre freshwater reservoir: state and variability from observation, J. Geophys. Res., 114, C00A10, doi:10.1029/2008JC005104, 2009. 2753, 2761

Rabe, B., Schauer, U., Mackensen, A., Karcher, M., Hansen, E., and Beszczynska-Möller, A.: Freshwater components and transports in the Fram Strait – recent observations and changes since the late 1990s, Ocean Sci., 5, 219–233, doi:10.5194/os-5-219-2009, 2009. 2751, 2753, 2755, 2756, 2757, 2761, 2766, 2786

Rabe, B., Muenchow, A., Johnson, H. L., and Melling, H.: Nares Strait hydrography and salinity field from a 3-yr moored array, J. Geophys. Res., 115, C07010, doi:10.1029/2009JC005966, 2010. 2762

Rabe, B., Karcher, M., Schauer, U., Toole, J., Krishfield, R., Pisarev, S., Kauker, F., Gerdes, R., and Kikuchi, T.: An assessment of Arctic Ocean freshwater content changes from the 1990s to 2006–2008, Deep-Sea Res. Pt. I, 58, 173–185, doi:10.1016/j.dsr.2010.12.002, 2011. 2752, 2763, 2766

Rennermalm, A. K., Wood, E. F., Weaver, A. J., Eby, M., and Derý, S. J.: Relative sensitivity of the Atlantic meridional overturning circulation to river discharge into Hudson Bay and the Arctic Ocean, J. Geophys. Res., 112, G04S45, doi:10.1029/2006JG000330, 2007. 2751

Rudels, B.: Constraints on exchanges in the Arctic Mediterranean – do they exist and can they be of use?, Tellus A, 62A, 109–122, doi:10.1111/j.1600-0870.2009.00425.x, 2010. 2757, 2765

Rudels, B., Björk, G., Nilsson, J., Winsor, P., Lake, I., and Nohr, C.: The interaction between waters from the Arctic Ocean and the Nordic Seas north of Fram Strait and along the East Greenland Current: results from the Arctic Ocean-02 Oden expedition, J. Marine Syst., 55, 1–30, doi:10.1016/j.jmarsys.2004.06.008, 2005. 2751

Schauer, U. and Beszczynska-Möller, A.: Problems with estimation and interpretation of oceanic heat transport – conceptual remarks for the case of Fram Strait in the Arctic Ocean, Ocean Sci., 5, 487–494, doi:10.5194/os-5-487-2009, 2009. 2785

Schauer, U. and Budéus, G.: Physical Oceanography during POLARSTERN Cruise ARK-XIV/2, Alfred Wegener Institute for Polar and Marine Research, Bremerhaven, doi:10.1594/PANGAEA.733424, 2010. 2784

Schauer, U. and Rohardt, G.: Physical Oceanography during POLARSTERN cruise ARK-XXI/1b, Alfred Wegener Institute for Polar and Marine Research, Bremerhaven, doi:10.1594/PANGAEA.742621, 2010. 2784, 2785

Schauer, U. and Wisotzki, A.: Physical Oceanography during POLARSTERN Cruise ARK-XX/2, Alfred Wegener Institute for Polar and Marine Research, Bremerhaven, doi:10.1594/PANGAEA.742660, 2010. 2784

Schauer, U., Fahrbach, E., Østerhus, S., and Rohardt, G.: Arctic warming through the Fram Strait: oceanic heat transport from 3 yr of measurements, J. Geophys. Res., 109, C06026, doi:10.1029/2003JC001823, 2004. 2756

Schlichtholz, P.: Climatological baroclinic forcing of the barotropic flow in the East Greenland current in Fram Strait, J. Geophys. Res., 110, C08013, doi:10.1029/2004JC002701, 2005. 2757

Schlichtholz, P. and Houssais, M.-N.: An overwiew of the θ-S correlations in Fram Strait based on the MIZEX 84 data, Oceanologia, 44, 243–272, 2001. 2756

Serreze, M. C., Barrett, A. P., Slater, A. G., Woodgate, R., Aagaard, K., Lammers, R. B., Steele, M., Moritz, R., Meredith, M., and Less, C. M.: The large-scale freshwater cycle of the Arctic, J. Geophys. Res., 111, C11010, doi:10.1029/2005JC003424, 2006. 2758

Steele, M. and Boyd, T.: Retreat of the cold halocline layer in the Arctic Ocean, J. Geophys. Res., 103, 10419–10439, 1998. 2751, 2753, 2765

Sutherland, D. A., Pickart, R. S., Jones, E. P., Azetsu-Scott, K., Eert, A. J., and Olafsson, J.: Freshwater composition of the waters off Southeast Greenland and their link to the Arctic Ocean, J. Geophys. Res., 114, C05020, doi:10.1029/2008JC004808, 2009. 2751, 2766

OSD
9, 2749–2792, 2012

Fram Strait freshwater exports 1998–2010

B. Rabe et al.

Talley, L. D.: Freshwater transport estimates and the global overturning circulation: shallow, deep and throughflow components, Prog. Oceanogr., 78, 257–303, doi:10.1016/j.pocean.2008.05.001, 2008. 2751

Taylor, J. R., Falkner, K. K., Schauer, U., and Meredith, M.: Quantitative considerations of dissolved barium as a tracer in the Arctic Ocean, J. Geophys. Res., 108, 3374, doi:10.1029/2002JC001635, 2003. 2762

Thompson, D. W. J. and Wallace, J. M.: The arctic oscillation signature in the wintertime geopotential height and temperature fields, Geophys. Res. Lett., 25, 1297–1300, 1998. 2752, 2764, 2783, 2792

Timmermans, M.-L., Proshutinsky, A., Krishfield, R. A., Perovich, D. K., Richter-Menge, J. A., Stanton, T. P., and Toole, J. M.: Surface freshening in the Arctic Ocean's Eurasian Basin: an apparent consequence of recent change in the wind-driven circulation, J. Geophys. Res., 116, C00D03, doi:10.1029/2011JC006975, 2011. 2762, 2763, 2765

Toole, J. M., Timmermans, M. L., Perovich, D. K., Krishfield, R. A., Proshutinsky, A., and Richter-Menge, J. A.: Influences of the ocean surface mixed layer and thermohaline stratification on Arctic Sea ice in the Central Canada Basin, J. Geophys. Res., 115, C10018, doi:10.1029/2009JC005660, 2010. 2762

Visbeck, M.: Deep velocity profiling using lowered acoustic Doppler current profilers: bottom track and inverse solutions, J. Atmos. Ocean. Tech., 19, 794–807, doi:10.1175/1520-0426(2002)019<0794:DVPULA>2.0.CO;2, 2002. 2754

Woodgate, R. A., Aagaard, K., and Weingartner, T. J.: Interannual changes in the Bering Strait fluxes of volume, heat and freshwater between 1991 and 2004, Geophys. Res. Lett., 33, L15609, doi:10.1029/2006GL026931, 2006. 2764

Yamamoto-Kawai, M., Tanaka, N., and Pivovarov, S.: Freshwater and brine behaviors in the Arctic Ocean deduced from historical data of δ^{18}O and alkalinity (1929–2002 AD), J. Geophys. Res., 110, C10003, doi:10.1029/2004JC002793, 2005. 2752

Yamamoto-Kawai, M., Carmack, E., and McLaughlin, F.: Nitrogen balance and Arctic throughflow, Nature, 443, 7107, doi:10.1038/443043a, 2006. 2752

Yamamoto-Kawai, M., McLaughlin, F. A., Carmack, E. C., Nishino, S., and Shimada, K.: Freshwater budget of the Canada Basin, Arctic Ocean, from salinity, δ^{18}O, and nutrients, J. Geophys. Res., 113, C01007, doi:10.1029/2006JC003858, 2008. 2755, 2764

Yamamoto-Kawai, M., McLaughlin, F. A., Carmack, E. C., Nishino, S., Shimada, K., and Kurita, N.: Surface freshening of the Canada Basin, 2003–2007: river runoff versus sea ice meltwater, J. Geophys. Res., 114, C00A05, doi:10.1029/2008JC005000, 2009. 2762, 2763

Zhang, D., McPhaden, M. J., and Johns, W. E.: Observational evidence for flow between the subtropical and tropical Atlantic: the Atlantic tropical cells, J. Phys. Oceanogr., 33, 1783–1797, 2003. 2751

Zhang, X., Sorteberg, A., Zhang, J., Gerdes, R., and Comiso, J. C.: Recent radical shifts of atmospheric circulations and rapid changes in Arctic climate system, Geophys. Res. Lett., 35, L22701, doi:10.1029/2008GL035607, 2008. 2752

Table 1. Glossary.

- AO: Arctic Oscillation (Thompson and Wallace, 1998)
- EGC: East Greenland Current
- AW: Atlantic Water
- MW: meteoric water (river runoff and precipitation)
- LFW: liquid freshwater (the sum of all components)
- SIM: sea ice melt
- IFB: brine from ice formation
- PW: Pacific Water
- FSIM: freshwater part of SIM
- FIFB: freshwater part of IFB
- FPW: freshwater part of PW
- NAOSIM: North Atlantic-Arctic Ocean Sea Ice Model

OSD
9, 2749–2792, 2012

Table 2. Data sources by year and campaign, showing references to available CTD and tracer (only 1998) data, where available; for $\delta^{18}O$, nitrate and phosphate data from other years, please contact the authors of this work. Where applicable, a full citation of the database entry in the PANGAEA database is given; otherwise, the publication, where data were first shown. Observations from 2004 are only used indirectly due to reconstruction of $\delta^{18}O$ values for 2005 from the corresponding relationship to salinity in 2004. All campaigns were carried out between June and September (see Dodd et al., 2012).

Year	Ship / Campaign	Reference	DOI or contact
1998	PS ARK-XIV/2	Schauer and Budéus (2010)	doi:10.1594/PANGAEA.759130
1998*	PS ARK-XIV/2	Fahrbach and VEINS members (2010)	doi:10.1594/PANGAEA.759130
(2004)	PS ARK-XX/2	Schauer and Wisotzki (2010)	doi:10.1594/PANGAEA.742660
2005	PS ARK-XXI/1b	Schauer and Rohardt (2010)	doi:10.1594/PANGAEA.742621
2008	PS ARK-XXIII/2	Beszczynska-Möller and Wisotzki (2010)	doi:10.1594/PANGAEA.733424
2009	LA Fram Strait 2009	Dodd et al. (2012)	Edmond.Hansen@npolar.no
2010	LA Fram Strait 2010	Dodd et al. (2012)	Edmond.Hansen@npolar.no

Entries marked with * refer to nitrate, phosphate and $\delta^{18}O$ water sample measurements, all others denote temperature and salinity (CTD) profiles.
Ship abbreviations are as follows: PS = R/V *Polarstern*; OD = R/V *Oden*, LA = R/V *Lance*.

OSD
9, 2749–2792, 2012

Table 3. Data sources by year and campaign, showing references to available velocity observations from the ship and from moorings, where available. Entries with a cruise label refer to ship-based observations, others refer to moored observations. At least one of the following references are given: a full citation of the database entry in the PANGAEA database; the publication, where data were first shown; the contact e-mail of the PI. Only the eastern part of the velocity data from moorings is in the PANGAEA database, so an e-mail contact is given in addition. The PANGAEA citations for velocity data from the eastern moorings are given in Appendix A. Ship abbreviations are the same as in Table 2.

Year	Ship / Campaign / instrument	Reference	DOI or contact
1998	PS ARK-XIV/2 vmADCP	Fahrbach (2005)	doi:10.1594/PANGAEA.318314
1998	Moorings	Fahrbach et al. (2001)	Appendix A and Edmond.Hansen@npolar.no
2005	PS ARK-XXI/1b vmADCP	Schauer and Rohardt (2010)	Hannelore.Witte@awi.de
2005	Moorings	Schauer and Beszczynska-Moeller (2009)	Appendix A and Edmond.Hansen@npolar.no
2008	PS ARK-XXIII/2 vmADCP	Beszczynska-Möller and Wisotzki (2010)	Hannelore.Witte@awi.de
2008	Moorings	Schauer and Beszczynska-Moeller (2009) Beszczynska-Möller et al. (2012)	Appendix A and Edmond.Hansen@npolar.no
2009	LA Fram Strait 2009 vmADCP	N/A	Edmond.Hansen@npolar.no
2009	LA Fram Strait 2009 ADCP	N/A	Edmond.Hansen@npolar.no
2009	Moorings	Beszczynska-Möller et al. (2012)	Appendix A and Edmond.Hansen@npolar.no
2010	LA Fram Strait 2010 lADCP	N/A	Edmond.Hansen@npolar.no
2010	Moorings	Beszczynska-Möller et al. (2012)	Appendix A and Edmond.Hansen@npolar.no

OSD
9, 2749–2792, 2012

Table 4. Observed volume transports of LFW components between 10.6° W and 4° E for each year. Transport values are given in mSv; in addition, mean values in "()" are given in $km^3 yr^{-1}$. Negative FSIM transports represent positive FIFB transports. Transport errors from the inverse analysis are also given. The combined errors from the inverse and the end-member equations for LFW components are discussed in Sect. 2.4. Only for FPW and PW transports do we expect a significant departure from the error of the inverse estimate, about twice the error given here for all years. There is a potential overestimate of MW transports and underestimate of FSIM transports in 2005 by about 25 % due to the reconstruction of $\delta^{18}O$ values from salinity data (see Rabe et al., 2009).

Year	LFW	MW	FSIM	FPW	PW
1998	105 ± 7	92 ± 7	-58 ± 5	70 ± 5	834 ± 60
2005	92 ± 7	169 ± 12	-87 ± 6	9 ± 1	100 ± 9
2008	98 ± 10	145 ± 15	-70 ± 7	23 ± 2	272 ± 30
2009	51 ± 5	63 ± 6	-22 ± 3	8 ± 1	108 ± 13
2010	113 ± 11	147 ± 16	-63 ± 8	28 ± 3	334 ± 40
Mean	92(2900)	123(3880)	−60(−1890)	28(880)	330(10400)

OSD
9, 2749–2792, 2012

Fram Strait freshwater exports 1998–2010

B. Rabe et al.

Title Page
Abstract Introduction
Conclusions References
Tables Figures
◀▌ ▐▶
◀ ▶
Back Close
Full Screen / Esc
Printer-friendly Version
Interactive Discussion

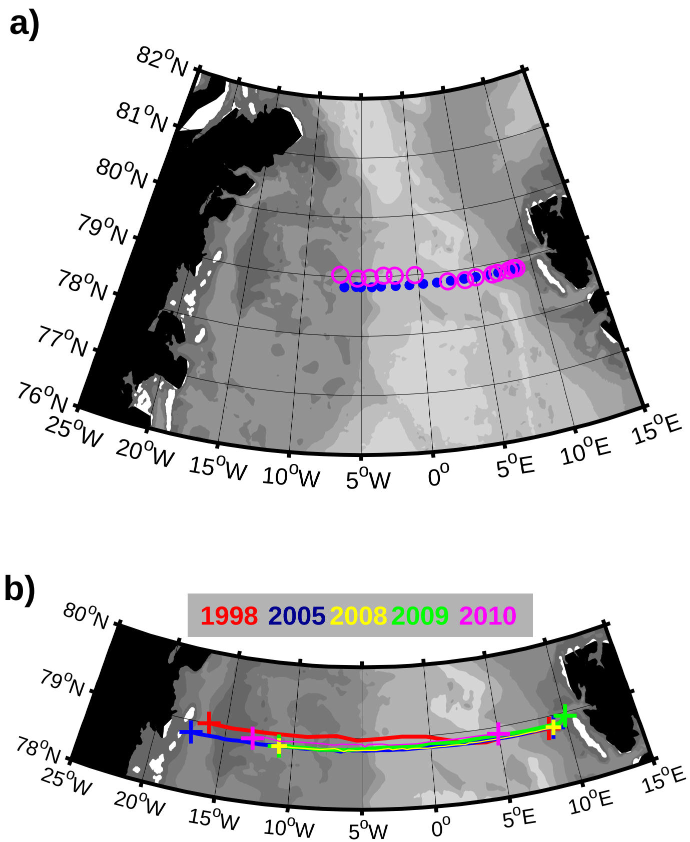

Fig. 1. Maps of **(a)** the locations of moorings for velocity measurements, for 1998 by circles, all other years by dots; **(b)** section lines for samples of δ^{18}O, nitrate and phosphate, where different years are indicated by colour as shown (see Fig. 2 in Dodd et al., 2012, for sampling locations along each section). Bathymetry shading in gray at intervals 100, 200, 1000, 2000 and 3000 m (from IBCAO, Jakobsson et al., 2008).

OSD
9, 2749–2792, 2012

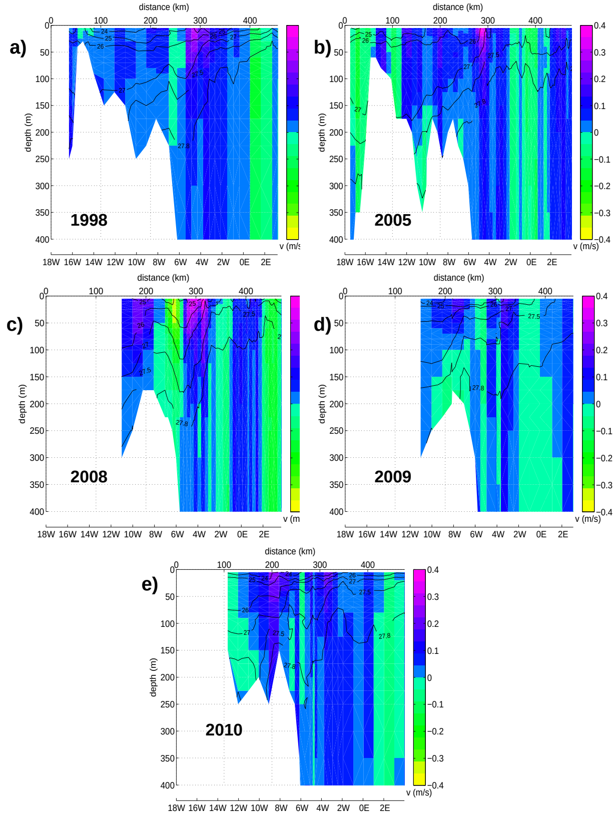

Fig. 2. Meridional velocity sections along the Western Fram Strait from the inverse solution: **(a)** 1998, **(b)** 2005, **(c)** 2008, **(d)** 2009 and **(e)** 2010. Velocity is positive southward. Contours represent potential density from the inverse solution. Potential density is given in σ notation, as departures from 1000 $kg\,m^{-3}$.

OSD
9, 2749–2792, 2012

Fram Strait freshwater exports 1998–2010

B. Rabe et al.

Title Page
Abstract | Introduction
Conclusions | References
Tables | Figures
◄ | ►
◄ | ►
Back | Close
Full Screen / Esc
Printer-friendly Version
Interactive Discussion

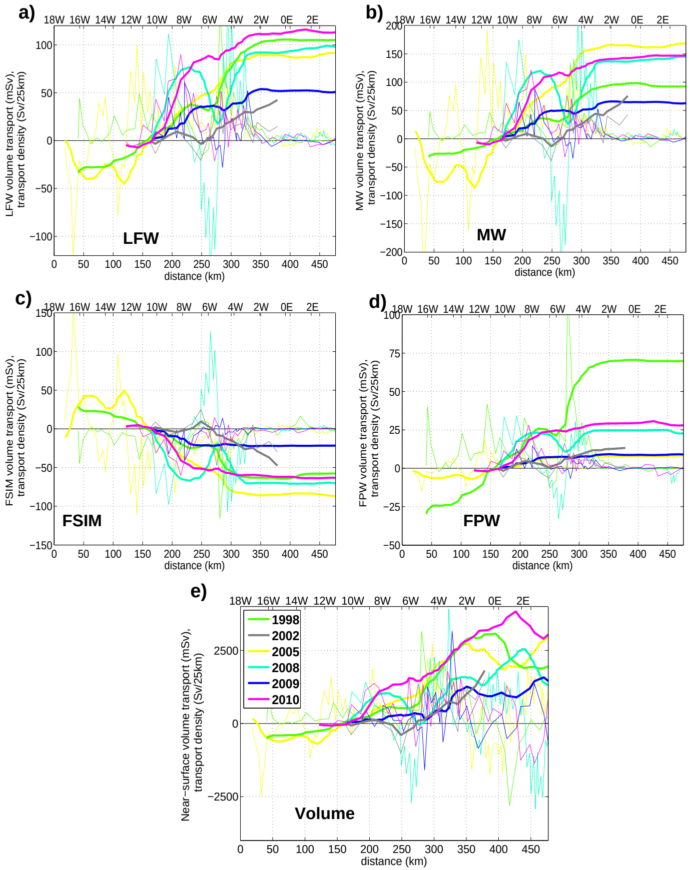

Fig. 3. Meridional volume transports of LFW components along the Western Fram Strait: **(a)** LFW, **(b)** MW, **(c)** FSIM (FIFB), **(d)** FPW. The volume transport in the upper 300 m is shown in **(e)**. Transport density is shown as thin lines and transports cumulated from 10.6° W as thick lines. Transports are positive southward. Results from different years are marked in color, according to the legend in **(e)**.

OSD
9, 2749–2792, 2012

Title Page
Abstract | Introduction
Conclusions | References
Tables | Figures
◄I | ►I
◄ | ►
Back | Close
Full Screen / Esc
Printer-friendly Version
Interactive Discussion

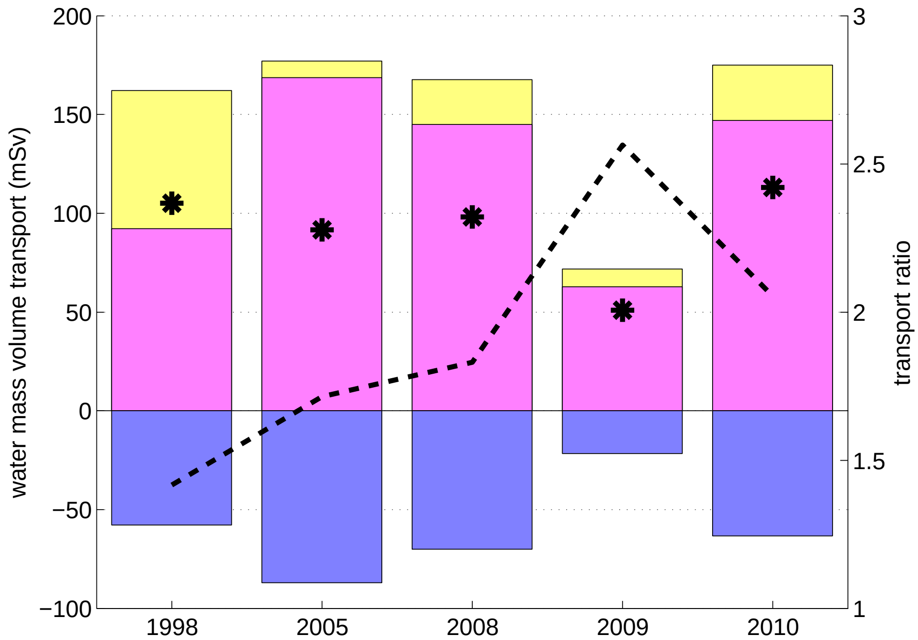

Fig. 4. Meridional volume transports of LFW and components in the Fram Strait between 10.6° W and 4° E for the years shown. The bars show the portion of every component: FPW (top, yellow), MW (magenta, middle) and FSIM (blue, bottom). The asterisks represent the LFW transport and the line the ratio of MW to FIFB transports.

OSD
9, 2749–2792, 2012
Fram Strait freshwater exports 1998–2010
B. Rabe et al.

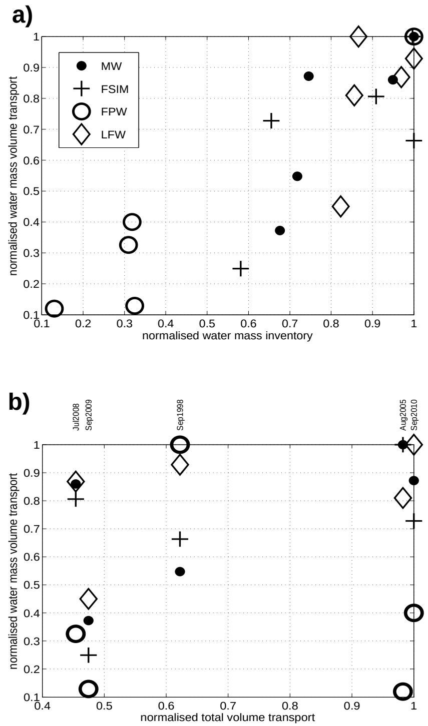

Fig. 5. Total meridional transports of LFW and components vs. section inventories of LFW and components **(a)**. LFW and component transports vs. volume transports in the upper 300 m **(b)**. Here, section inventories and section transports were calculated between 10.6° W and 4° E; the inventories are based on the fractions of LFW components in Dodd et al. (2012). All values are normalised by the respective maximum of all five campaigns. Inventories and transports of FSIM were multiplied by −1 (FIFB inventories and transports). Symbols denote different transport components: MW (dots), FSIM (plus), FPW (circles) and LFW (diamonds).

OSD
9, 2749–2792, 2012

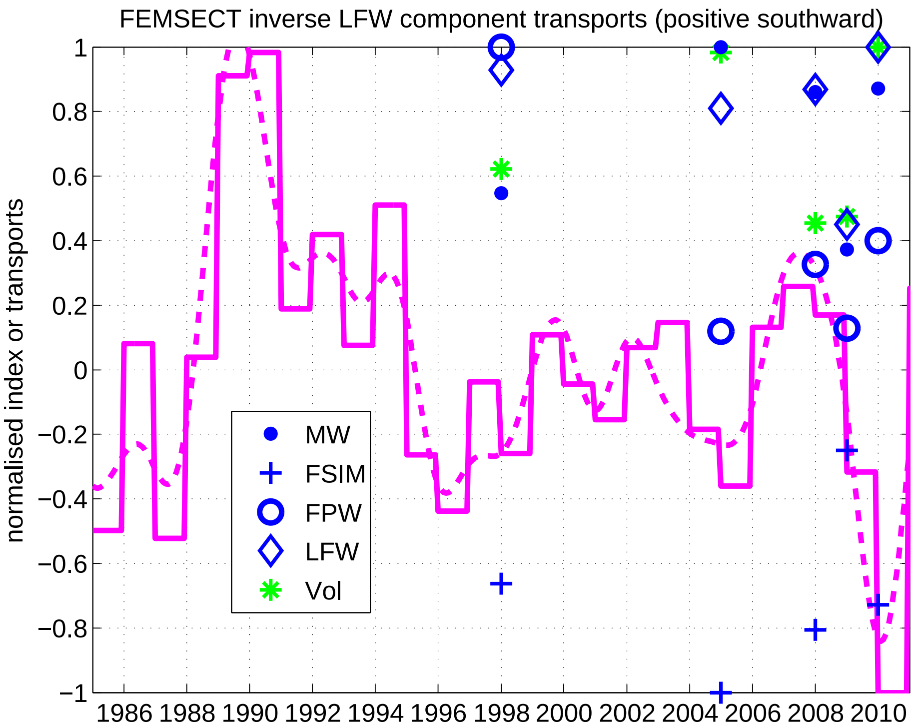

Fig. 6. Observed volume transports (green asterisks) and LFW component transports (blue; MW, dots; SIM, crosses; FPW, circles; LFW, diamonds) and the Arctic Oscillation index (Thompson and Wallace, 1998): annual mean (solid line) and 3 yr low-pass filtered monthly values (dashed line). All values are normalised by their absolute maxima.

OSD
9, 2749–2792, 2012

Fram Strait freshwater exports 1998–2010

B. Rabe et al.